Stony Brook University

Deformation Behavior of Honeycomb Foams in Compression

A Thesis Presented

by

Doo Hee Lee

to

The Graduate School

in Partial Fulfillment of the

Requirements

for the Degree of

Master of Science

in

Materials Science and Engineering of Degree Program

Stony Brook University

May 2014

Stony Brook University

The Graduate School

Doo Hee Lee

We, the thesis committee for the above candidate for the

Master of Science degree, hereby recommend

acceptance of this thesis.

Dr. T A Venkatesh – Thesis Advisor
Associate Professor, Materials Science and Engineering

Dr. Maen Alkhader – Thesis Co-advisor
Assistant Professor, Mechanical Engineering

Dr. Balaji Raghothamachar – Third Reader
Research Assistant Professor, Materials Science and Engineering

This thesis is accepted by the Graduate School

Charles Taber
Dean of the Graduate School

Abstract of the Thesis

Deformation Behavior of Honeycomb Foams in Compression

by

Doo Hee Lee

Master of Science

in

Materials Science and Engineering of Degree Program

Stony Brook University

2013

In the present work, poly lactic acid (PLA) is used as a model system to investigate the deformation behavior of honeycomb foams under compression loads. Solid PLA tension specimens and foams made of PLA were fabricated using fused deposition 3-D printing technique. The solid PLA tension specimens were characterized for their densities and found to be about 10% lower in density as compared to their bulk counter parts. The honeycomb foams had a relative density of about 47%. The deformation mechanisms leading to the crushing of the honeycomb foams under compression were characterized. Furthermore, simple finite element models were developed to understand the observed deformation behavior of honeycomb foams.

Table of Contents

List of Figures

List of Tables

Acknowledgments

I would like to express my special appreciation and thanks to my advisor Professor Dr. T A Venkatesh, who gave me warm encouragement and constructive comments for my research. And I would like thank Dr. Maen Alkhader for persistent invaluable guidance about research. I learned a lot from both of you, and without your guidance, this paper would not have been possible. Needless to mention that Mr. Pratap, co-researcher as well as my best friend, who has been a source of inspiration and for his passionate cooperation in the conduct of research. Words cannot express how grateful I am. I would like thank to Dr. Balaji Raghothamachar for being my committee. I also would like to thank Sumanthu for his valuable assistance. Last but not the least, I would like to thank my family.

Chapter 1 Introduction

Cellular materials have been applied as a shock absorber in impact or crash, due to their constitutive property, such as a high densification strain at the plateau stress under the plastic deformation. [3] Environmentally, cellular material is also being viewed as potentially beneficial, since cellular manufacturing helps by a reduction of waste and eliminating of overproduction according to the Environmental Protection Agency.[5] Cellular material also has been utilized as a scaffolds in bone tissue engineering, which is three dimensional biocompatible structures that can function as an extracellular matrix. [4]

As one of the cellular materials, honeycomb structure has a high relative strength and stiffness, heat insulation, and energy absorption as well. Especially, if it is subjected to out-of-plane crash, shows great energy absorption property, therefore, a lot of researches have done with out-of-plane of honeycomb structure.[4] However, the impact from various direction can happen, for example, from space debris crash on a space shuttle to the daily life impact. So, the investigation of in-plane property of cellular materials, honeycomb, also plays pivotal role in predicting the impact behavior. On this paper, quasi-static experiment of honeycomb was performed to characterizing mechanical property of the honeycomb structure printed by Poly Lactic Acid.

Three dimensional printing method is the technique for manufacturing haptic product from digital CAD file. By using 3D printer, nowadays people easily can access a production of prototype before massive manufacturing, hence also referred to rapid tooling. Even in medical area, the demand for 3D printing technique will increase in near future, since with 3D printing, custom medical devices can be made for patient specific and defect specific clinical needs. [1]

Especially, Fused Deposition Modelling (FDM) has become one of famous and widely used technique for a variety of applications, such as designing and introducing new materials, including

composites. This technique utilizes the fused material deposition on the base plate. For the fused material, referred to a filament,' the ABS(Acrylonitrile butadiene styrene) , PC(Polycarbonate), PPSF(Poly phenyl sulfone) and PLA(Poly Lactide). [2]

One of the main problem of using non-biodegradable plastic is the disposal when the product life cycle ends; hence, the demand of biodegradable polymer is emerging as an alternative solution. Poly Lactic Acid is becoming popular with great properties such as low toxicity, high mechanical strength, good barrier property, and biodegradability as well. [6]

The investigation of high strain rate behavior has been applied to a wide range of area for prediction of the auto-vehicle accident, airplane crash (even bird ingestion in jet engines), and spacecraft impact (such as meteorite or collision on satellites), loading to the building structures during an earthquake, and armor and projectile interactions. Split Hopkinson Pressure Bar apparatus is one of the best experiment technique to able to achieve the highest uniaxial stress loading of a specimen uniformly in compression at strain rates, which ranges from 10^2 s^{-1} to $10^4 s^{-1}$ generally. [32]

In this paper, to figure out the mechanical behavior of cellular material (honeycomb) printed by FDM 3D printing method, the quasi-static experiment and finite element analysis is performed. And also the characteristic of ‘printed PLA’ was investigated for the experiment of honeycomb.

Chapter 2 Background

2.1. 3D Printing

Three-dimensional printing technology is a methodology using 3D CAD (Computer Aided Design) data for manufacturing 3D haptic physical model. 3D printing is also called as a layered manufacturing, solid freeform and rapid prototyping depending on the type of production way.

The history of 3D printing method starts from early 90s by SACHS ETAL. [7] With a regular inkjet printer's head, powder based freeform production method was utilized and in a powder bed, printed on to loose powders. At the time, the purpose of 3D printing technique was rapid tooling for metals and ceramics. [8] The advantage of additive fabrication is its ability to create any complex shape or geometric feature.

2.1.1. Fused Deposition Modelling (FDM)

Fused Deposition Modelling, which is one of most famous 3d printing method, can manufacture parts with a range of materials including elastomers, PLA (Poly Lactic Acid), and ABS (Acrylonitrile Butadiene Styrene) and so on. Once FDM printer is operated, the rolled filament (PLA in fig.1) is fed up to the head through the hose. So the filament is molten by heated element in the head at the temperature around 230 degree Celsius. And then the FDM measure the distance between head and the work plate where the filament is extruded. And then it is extruding the molten PLA onto the work plate layer by layer. The CAD file is automatically sliced by FDM software, then the printer use the converted slice data. The thickness of the line of molten filament could be set before printing out. The head (fig.2) travels on the X and Y plane, and emitting the PLA from the layer data. When a printing out a layer is finished, the plate moves down vertically in Z-axis

to destined height. And then the head is moving in X-Y plane, and extruding the filament on top of the previous one.

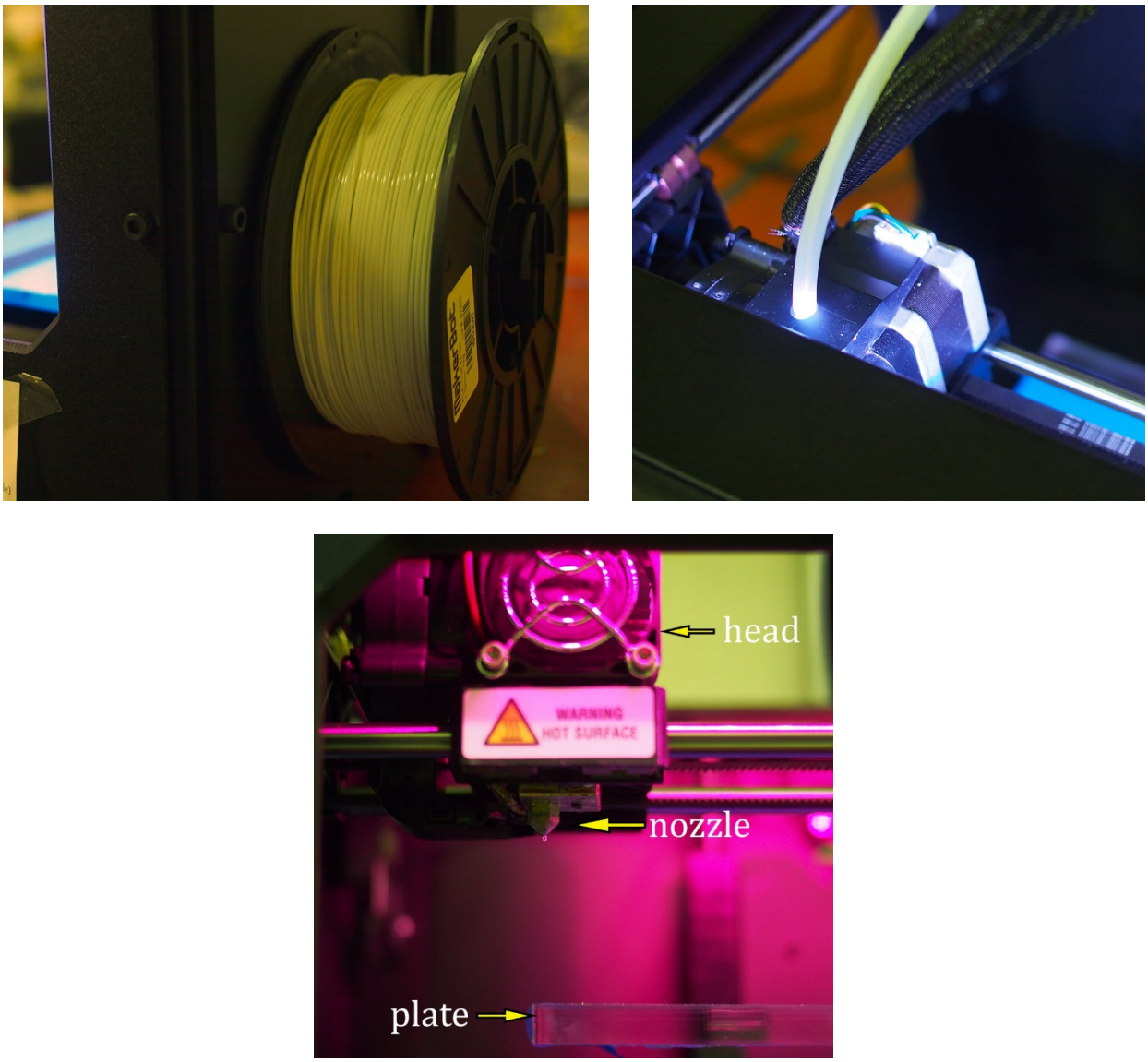

Fig.1 - (a) A roll of PLA filament, (b) the hose which is linked to the head, and (c) The head, nozzle and construction plate of FDM printer.

2.1.2. Limitation and conclusion

However, the 3D printing technique, or FDM, has also limitations. The output should be smaller than work chamber. Hence, if the full body of product is larger than 3D printer, the separated modelling is required. The assembly of the separated part is next step.

The application of 3D printing method is increasing. Even in medical area, due to their ability to make custom medical tools that can be tailored for each patient and clinical needs, demand for 3D printing technique will be developed further. [1]

To meet the future demands for designers, artists and entrepreneurs hoping to manufacture more complicate and high technology output using 3D printing method, the incorporation of functional apparatus such as electronic sensor into 3D printed macro-scale structures is also suggested. [9] In order to come into wide application of 3D printing technique, low-cost and easy to access functional materials are required.

2.2. Poly Lactic Acid

2.2.1. Introduction of PLA

Poly-Lactic Acid (PLA) or poly-lactide was found in 1932 by Carothers. At the time, He only could manufacture a low molecular weight poly-lactide by heating lactic acid under vacuum condition while eliminating the condensed water. Increasing the molecular weight of the PLA was difficult at that time. However, finally high-molecular weight Poly-lactide was synthesized by ring-opening polymerization of the lactide. Poly-Lactic Acid was firstly applied in combination with poly-glycolic acid (PGA) as a suture material. And it was sold with being called as 'Vicryl' in the United States in 1974.[10]

One of the main problem of using non-biodegradable plastic is the disposal when the product life ends, hence, the demand of biodegradable plastic is emerging as an alternative solution. Poly Lactic Acid is becoming popular with great properties such as low toxicity, high mechanical strength, good barrier property, and biodegradability as well. [6]

Poly Lactic Acid is grounded on agricultural, biological, and chemical technologies, respectively representative of crop, fermentation, and polymerization. It is categorized as 'Generally Recognized As Safe' (GRAS) by the United of States FDA. [11]

2.2.2. Fabrication of PLA

The single monomer of Poly lactide is 2-hydroxy propionic acid (Lactic acid)(fig.2), which is manufactured by fermentation and chemical synthesis. Industrial Lactic acid production prefers to use the lactic fermentation procedure than synthesis because the synthetic processes have many

important limitations. Limited capacity, because of the dependency on a byproduct of another procedure and high producing costs are those problems. [12]

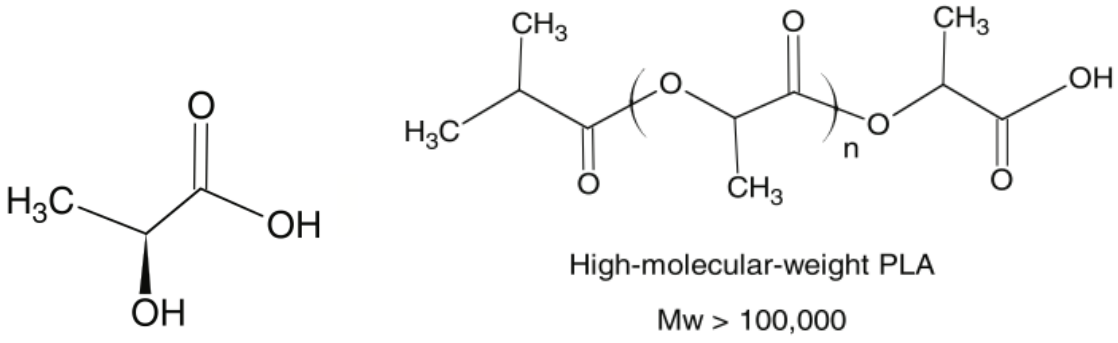

Fig.2 - (a) Lactic Acid and (b) high molecular weight Poly-Lactic Acid.

There are generally three ways for the polymerization of lactic acid.

(1) Direct condensation polymerization.

(2) Direct polycondensation in an azeotropic solution. (An azeotrope refers to a mixture of two or more chemical liquids with a ratio that its composition cannot be altered by simple distillation.)

(3) Polymerization through lactic acid formation. [13]

Compared to other hydrocarbon based polymers most positive benefit is the reduction of CO2 emission. CO2 is considered as one of the biggest reason of global warming. Since CO2 is absorbed while corn is grown, application of Poly lactide can mean fewer emission of CO2 which making the earth greenhouse than other hydrocarbon based polymers. [10]

PLA exhibits thermally unstable and rapid loss of molecular weight during thermal treatment at controlling temperatures. Poly lactide experiences thermal degradation even at temperature lower

than the polymer's melting point, and the degradation rate significantly increases above the melting point. [10]

Poly Lactic Acid has various characteristic properties such as high mechanical strength, low toxicity, good barrier properties and good appearance as well. (, though the barrier property of Poly Lactic Acid, the coefficient of permeability of CO2 and O2 was lower than the coefficients of PS and PET.)

2.2.3. Application

PLA has applied to a wide range of area. The degradability and the fact that it is made by renewable resources are not only reasons to use PLA material. The PLA's great properties and functionality are making it used to lots of industries. The application of Poly Lactic acid also reaches in biomedical area for the internal body parts.

For example, interference screws for knee, pins for ligament, pins and rod in a bone, bone fixation screws. Furthermore, for implants, surgical sutures, and drug delivery medium are the application of PLA. [14] [15]

2.2.4. Degradability and limitation of PLA

Almost all plastics have resistance to microbial attack. But, on the other hand, PLA is degraded easily by microorganisms exist in nature. By the definition from the ASTM D6400-04, a biodegradable plastic means that 'a plastic that degrades because of the action of naturally occurring microorganisms such as bacteria, fungi, and algae."

PLA degradation in the environment is not easy since PLA is also resistant by microorganisms in the soil. So, to reduce the molecular weight before biodegradation the polymer must firstly be hydrolyzed at increased temperatures (approximately 58◦C.) Brandrup and Ohkita reported that

degradation was not found on PLA sheets even after 6weeks in soil, hence poly lactic acid will not degrade in general garden fertilizer. [16]

Compared to other petrochemical polymers, the production cost of PLA was disadvantage, but on these days, by optimizing PLA production procedure, cost of the PLA is decreasing day by day as demands of PLA increased.

Bastioli reported that beyond the global demand for biodegradable plastics will keep increasing by 30% every year and PLA will be large portion of the plastic business due to its reasonable properties. [17]

However, the some properties would limit its applications, which is its brittleness and higher permeability compared to other plastics, low heat distortion temperature, toughness and high cost.[18] Hence, the modification of develop PLA's properties is needed and expected.

2.3. Cellular material

2.3.1 Introduction of cellular structure

Cellular materials, such as metal foam and honeycomb structures, are applied as absorbers of impact energy in crash because of their unique constitutive property, which is large densification strain ε_D at the plateau stress σ_{pl} during the plastic compression. [3]

There are generally three stages that could be defined in the stress-strain-stress curve of the cellular material under uniaxial compression. Fig.3 is shown schematically.

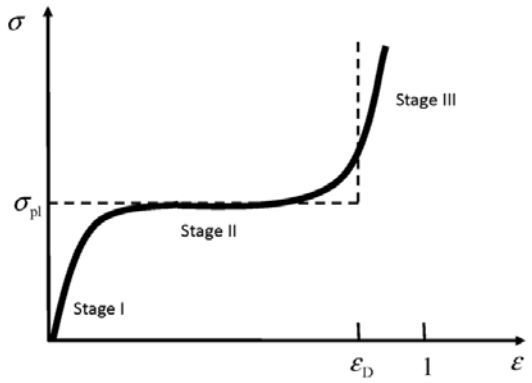

Fig.3 - Constitutive behavior of general material. The solid line refer to strain-stress curve and the dashed line refers to the idealization of the curve in the rigid, perfect plastic, locking model. (RPPL)

Stage 1 - Reversible deformation as the bending of the cell walls takes place for a closed-cell cellular material. Some cells collapse at the end of stage 1. Plastic deformation, elastic buckling or fracture can be the reason of the collapse.

Stage 2 - the constant compressive stress shows in a long range of strain. Until all cells are completely collapsed, plastic and buckling collapse takes place continuously and the deformation that is in ‘stage 2’ is irreversible.

Stage 3- Cell walls are crushed each other, which cause a steeply rising stress.

The dashed line in Fig.3 is a simplified rigid, perfectly-plastic, locking model (RPPL) which is firstly dealt by Reid and Peng. [19] The constitutive property at stage 1 is simplified as rigid. Stage 2 is dealt as perfect-plastic with the yielding plateau stress σ_{pl}, and ends with the densification (locking) strain ε_D. 'Stage 3' is again simplified as rigid.

To design the cellular materials as a shock absorber in crush or blast, understanding of the wave behavior in the materials is needed. After being impacted by a striker, two waves are produced along the cellular rod, elastic wave and then a plastic shock wave. But, for the stage of the plastic shock wave, the impact velocity V_m should be higher than a critical velocity V_m^c. [3]

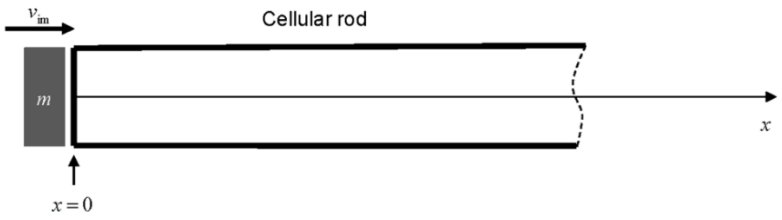

Fig.4 - One dimensional uniaxial compression model having with impact from the striker of mass 'm' and velocity '$v_{m.}$'[3]

In bone tissue engineering area, scaffolds are three dimensional biocompatible structures which is designed with cellular pattern. It can imitate the characteristic of the extracellular matrix (ECM), such as mechanical support, protein production through mechanical and bio-chemical interactions, and cellular activity, so on), and provide a template for cell attachment. [5]

Environmentally, cellular material is also being viewed as potentially beneficial, since cellular manufacturing helps by a reduction of waste and eliminating of overproduction according to the Environmental Protection Agency.

2.3.2. Introduction of honeycomb

Cellular materials have been suggested for use in shock mitigation and energy absorption of impact. [21] Cellular materials shows the noticeable characteristic of the compression behavior, called localization.

Among the cellular material, honeycomb structure has paid attention for the great properties in high relative strength and stiffness, heat insulation, and an energy absorption.

For the wide area of application the aluminum honeycomb in the sandwich structure being utilized, such as wind energy systems, airplane, ships, and auto vehicle as well. For a skin, high strength multi-layered material has been used and inside of the skin the low density cellular material is applied.[20]

2.3.3 Quasi-static behavior of honeycomb

M.R. Said [20] reported that the deformation of honeycomb in quasi-static compression can be categorized into three zones.

• Zone 1 is the beginning stiff, elastic state.

• Zone 2 is the plateau part of the stress-strain curve at which collapsing of lines of cells happens at an almost constant load, with minuscule non-uniform force oscillation.

• Zone 3 is the end of plateau part and presents a stiffening region related with densification of the material. [20]

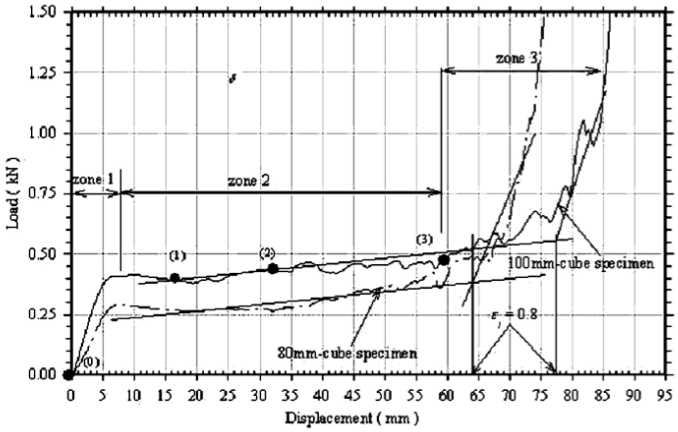

Fig.5 - Example of load-displacement graph of laterally compressed (across corners) 100 mm- cube and 80 mm-cube honeycomb material on quasi-static experiment. [20]

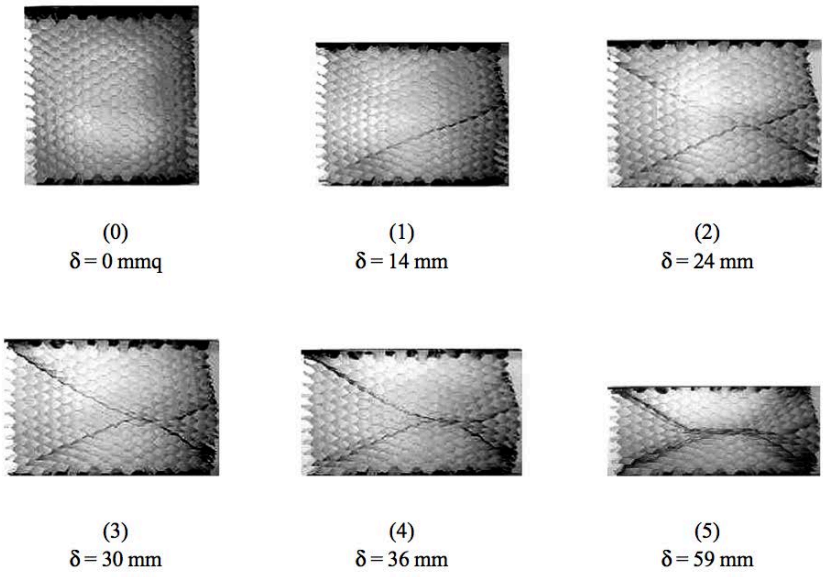

Fig.6 - Photos of a general specimen experiencing the deformation on quasi-static experiment. [20]

2.3.4. Dynamic behavior

When the honeycomb structure is exposed to out-of-plane impact, it has the great energy absorption which is why lots of research are concerned about the out-of-plane property. But, based on the situation that could be tough, crushing could occur along various direction of honeycomb. So, the investigation of in-plane dynamic property of a honeycomb is required as well as out-of-plane behavior.[4]

Collapse happens at the weakest band or row of cells for the first time and then dispersed to area that is stronger of the structure. From numerical simulations [22] when honeycombs are exposed to uniaxial impact, three characteristic patterns of localization could be identified: X, V and I pattern.(Fig.7)

'X' pattern occurs under lower impact velocity (order of 1m/s) and could be referred to quasi-static localization mode. And 'I' pattern occurs under higher impact velocity (on the order of 100m/s), referred as dynamic localization mode. Last of all, 'V' pattern is a transition status between those. [4]

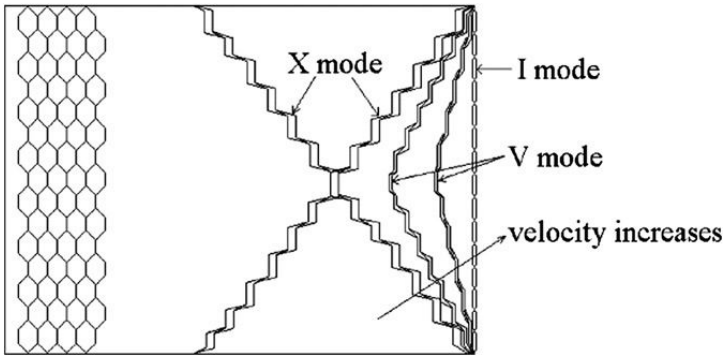

Fig.7 - Three types of deformation in honeycomb structure [4]

If the velocity of impact is high, the localization row will develop in the 'dynamic localization mode' (I-pattern in fig.7) and then spread layer by layer from the end of impact to the other end.

This spreading densification can be refer to ‘structural shock’ in cellular materials. The propagation of a shock wave in continuum is similar with this phenomenon.

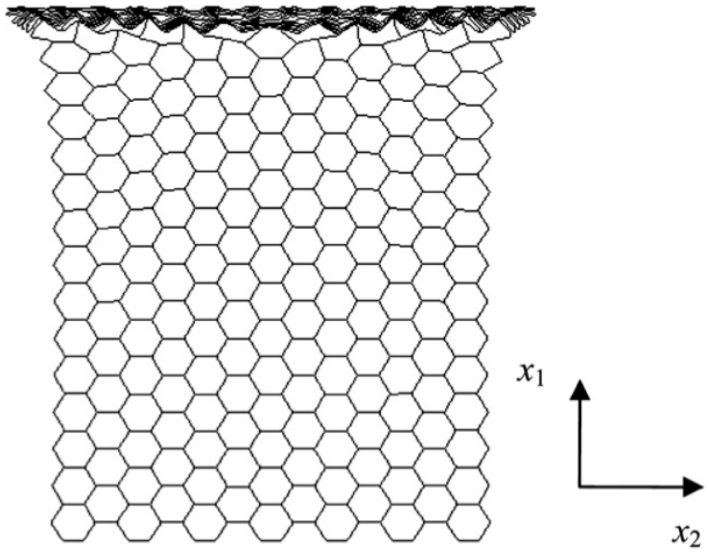

Fig.8 – the dynamic localization mode. [4]

Ruan et al. [22] formulated an empirical equation to get A about h/l, by using FE simulations at high velocity impact.

$$\sigma_d = \sigma_0 + \frac{\rho^*}{\varepsilon_d} V^2 = \sigma_0 + AV^2 \quad (1)$$

In eq.(1), *‘σ_d’* and σ_0 are the crushing strengths of the cellular structured material under dynamic crushing and under quasi-static compression respectively.

‘ρ^*’ refers to the initial density of the cellular material, which is a function of the ratio between the thickness of cell wall ‘*h*’ and the length of cell wall ‘*l*.’ *‘ε_d’* refers to the densification strain (locking strain) under quasi static compression, which is derived from the stress-strain curve of the cellular material under quasi static uniaxial compression. ‘*V*’ is the impact velocity. *‘A’(= ρ^*/*

ε_d) is a material parameter. Because the *'ρ*'* and *'ε_d'* both are changed with the thickness of cell wall with ratio h/l, *'A'* should be a function of '*h/l'*, too.

L.L. Hua and T.X. Yu[4] investigated the effect of the unequal thickness of the cell walls of honeycomb structure when it tis exposed to dynamic crushing strength, and found that the dynamic crushing strength of the double-thickness honeycomb is approximately 1.3 times higher than the single-thickness honeycomb. [4]

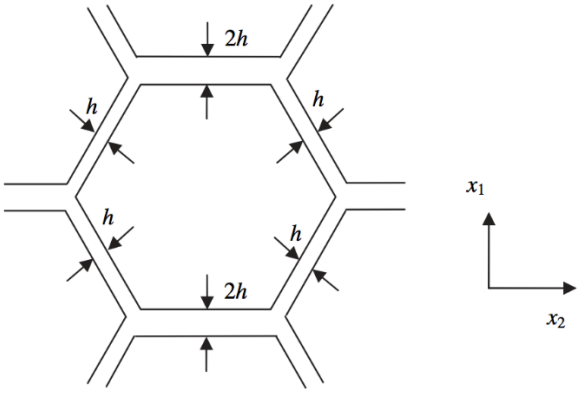

Fig.9 – Example of schematic of double cell honeycomb. [4]

Z.ZOU[21] simulated the dynamic crushing of honeycomb structure by using finite elements.

Cell collapse usually starts at the fixed and impact ends, if exposed to low crushing speed.

And then the deformation propagates to the center of the honeycomb through the collective multiplication of discrete bands. With the crushing velocity increases over a critical value affiliated with the steady shock velocity, collapse of cell initiates at the impact end and develop progressively to the fixed end with a shock-like manner. The critical crushing velocity differ to the relative density of the honeycomb with equation (2).

$$V \geq V_s = \sqrt{2\sigma_0 \varepsilon_d / \rho}. \quad (2)$$

Characteristic shock thickness related with the spreading shock front at supercritical velocities, at which the deformation mode transits, which is around one cell diameter exists. If it is superficial, the thickness is almost independent of relative density of honeycomb and the crushing velocity, though the amount of the critical compression velocity increases with the relative density of the honeycomb. From the results from the finite element analysis by Z.Zou [21], crushing velocity increases both the crushing stress and the plastic energy dissipation density. Once the crushing velocity is sufficiently high to make a chock in the honeycomb structure, both the plastic energy and crushing stress are associated to the crushing velocity by a square law. As crushing velocity increases, densification strain also increases. [21]

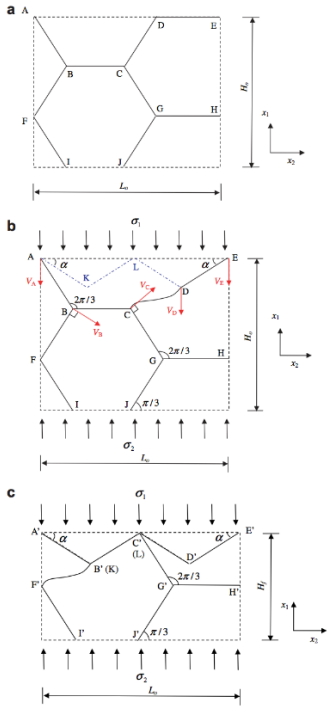

Fig.10 - The example schematic of dynamic impact of honeycomb structure; (a) An area before deformation; reference area, (b) the initial shape of the reference area at initial stage of collapse process, (c) the final shape of the reference area at the end of stage of collapse procedure. [4]

2.4. Split Hopkinson Pressure Bar experiment

2.4.1. Introduction of SHPB

Historically, compared to static experiment, high-strain experiment has little been paid attention. Concern in the high rate mechanical property of materials has increased during the last four decades, which is from the demands for cumulative knowledge of material reaction in impact events. The investigation of high strain rate behavior has been applied to a wide range of area for prediction of the auto-vehicle accident, airplane crash (even bird ingestion in jet engines), and spacecraft impact (such as meteorite or collision on satellites), loading to the building structures during an earthquake, and armor and projectile interactions. Split Hopkinson Pressure Bar apparatus is one of the best experiment technique to able to achieve the highest uniaxial stress loading of a specimen uniformly in compression at strain rates, which ranges from 102 s-1 to 104s-1 generally. From the impact event the stress wave are generated, and stress is measured via an elastic element in a series along the specimen. [32]

2.4.2. History

Bertram Hopkinson (1914) invented the Hopkinson bar technique to measure the pressure produced by using the induced wave spread in a long elastic bar during dynamic events in 1914.

Hopkinson investigated the shape of stress waves as they travel along rods as a function of time through the application of momentum traps of different lengths. Based on Hopskin's previous work, the Hopkinson bar was named as the Hopkinson Pressure Bar, which was used to investigate the dynamic processes. Davies (1948) and Kolsky (1949) applied two separate bars in series with locating the sample in between the two bars to study the dynamic stress-strain response of the specimen. After their work, the apparatus has been named as the Split Hopkinson Pressure Bar.

[23] [32] The SHPB has experienced many modifications. It was applied for tensile tests (Lindholm, 1968), torsion tests (Bassim,1999), simultaneous compression and also torsion (Lewis, 1973), and fracture dynamics (Klepaczko, 1979.) [29] By allowing the execution of compression tests after tension and the investigation of the Baushinger effect at high strain rates, Nemat-Nasser et al. (1991) invented novel technics to the SHPB. He also introduce the technique that allows the execution of dynamic recovery experiments where the material is exposed to a pre-assigned stress wave and then recovered without further loading for post-test microstructure study. Noticeably, SHPB experiment at high temperature also was tried by Muller. (1972) [29]

2.4.3. Principle of SHPB

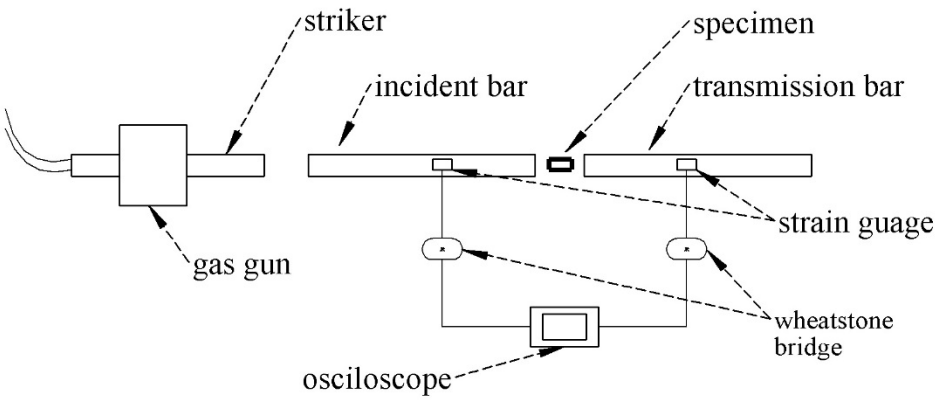

Fig.11 - A schematic of Split Hopkinson Pressure Bar.

Split Hopkinson Pressure Bar apparatus is composed of incident bar and transmission bar (two main split bar of SHPB), striker bar (for implying impact to incident bar), and gas gun for projection of striker bar. And striker bar, incident bar and transmission bar should be aligned serially. The Fig.11 shows a schematic of conventional Split Hopkinson Pressure Bar experiment apparatus.

When striker bar, which is operated with gas gun, impact the incident bar with a predetermined speed, the stress pulse, which is generated by impact, travels through the incident bar and specimen that is placed between incident bar and transmission bar. Two strain gauges are located at each middle of incident bar and transmission bar. With the ‘wheatstone bridge’ circuit, the data of voltage is collected, then amplified to the oscilloscope. With this procedure, the stress-strain curve of the specimen could be gain. High speed camera is located in front of the specimen to track the visible deformation of specimen with a function of time.

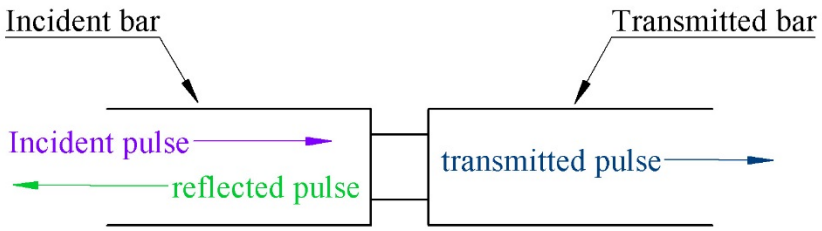

Fig. 12 - The direction of incident, reflected and transmitted pulse. (, modified from [31])

There are three waves (pulses) in SHPB apparatus. When striker bar gives impact to the incident bar, the stress wave travels along incident bar at the end of the bar, which is referred to ‘incident wave.’ However the mismatch of impedances between specimen and incident bar makes reflection of some portion of the incident wave and it is called ‘reflected wave.’ (Fig.12) The rest of the incident wave (excluding reflected wave) pass through the specimen, making the specimen compressed with high strain rate, to transmission bar, which is called ‘transmitted wave.’ Fig.12. shows the direction of three waves schematically. These three signals are sensed by two strain gauges located at each bars and then recalculated into the digital oscilloscope. [30]

To guarantee better data interpretation (for minimizing the unreliablility,) SHPB should meet some requirements. The lengh of SHPB must be enoughly long with a comparison of the length

of the incident wave in order not to overlap the waves, and the bars should remain elastic.[24] Small diameter of bar is suitable for minimizing the two dimensional stress wave prpogation inside the bars. The ends of the bar which hits the specimen should be flat and be parallel with the specimen during the test.[24] Lastly, the crosssectional area of the specimen must be lower than that of bars.

The $\varepsilon_i(t)$, $\varepsilon_r(t)$ and $\varepsilon_t(t)$ are refered as incident, reflected, and transmitted strain histories, respectively, measured by strain guage. And A_0 is the cross-sectional area of the bars. E_0 is young's modulus and C_0 is the wave speed of elastic bar. A_s and L_s are original crosssectional area and length of the specimen.

From the one dimensional stress wave analysis on the bars shows the strain rate, strain, and stress histories in the specimen, respectively [24].

$$\dot{\varepsilon} = \frac{C_0}{L_s}[\varepsilon_i(t) - \varepsilon_r(t) - \varepsilon_t(t)] \tag{1}$$

$$\varepsilon = \frac{C_0}{L_s}\int_0^t [\varepsilon_i(t) - \varepsilon_r(t) - \varepsilon_t(t)]dt \tag{2}$$

$$\sigma = \frac{A_0}{2A_s}E_0[\varepsilon_i(t) + \varepsilon_r(t) + \varepsilon_t(t)] \tag{3}$$

If the specimen is at the state of uniform stress,

$$\varepsilon_i(t) + \varepsilon_r(t) = \varepsilon_t(t) \tag{4}$$

And Eq.(1), (2) and (3) are simplified to eq(5), (6) and (7), respectively.

$$\dot{\varepsilon} = -2\frac{C_0}{L_s}[\varepsilon_r(t)] \tag{5}$$

$$\varepsilon = -2\frac{C_0}{L_s}\int_0^t \varepsilon_r(t)dt \tag{6}$$

$$\sigma = \frac{A_0}{A_s}E_0\varepsilon_t(t) \tag{7}$$

With the procedure the stress-strain data can be obtained from the recorded strain histories from the strain guage.[23]

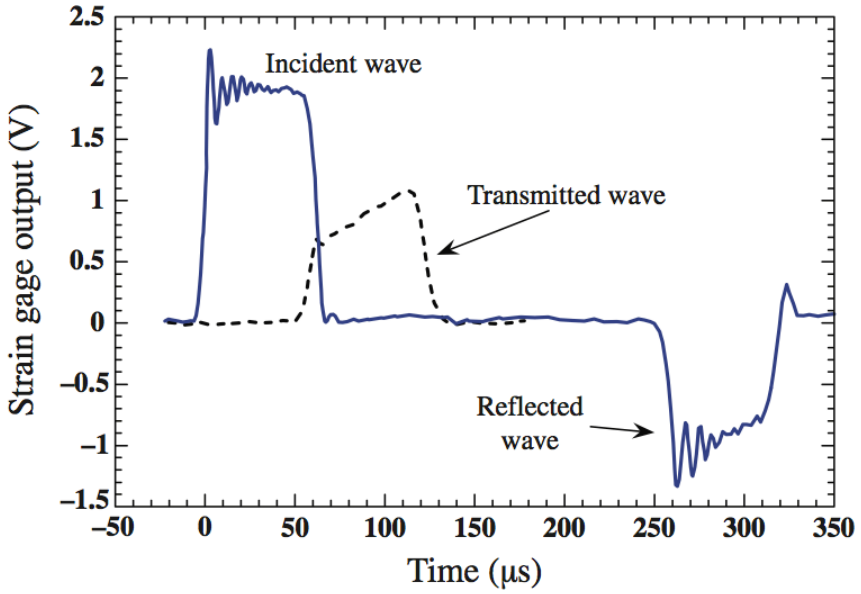

Fig.13 - An eaxample of three waves measured by strain guage in SHPB. [32]

Fig.S3 shows the sample data by Split Hopkinson Pressure Bar with a nickel alloy specimen. There are three pulses measured as a function of time. In Fig.13, transmitted wave is intentionally added over the other waves. [32]

After stress-strain curves are provided from SHPB dynamic experiment, after mechanicl loading to the specimen, microstructural investigations of damaged spcimen are sometimes desired to study the deformation of the specimen inside. [25][26]

M. Prot[33] investigated the bovine cancellous bone spcimen after SHPB experiment microstructurely. To investigate microstructure of bone, several steps operated : embedding specimens in a resin as a medium and then sectioning of the resin embedding the bone with a diamond cutter, grinding surface to attach to a slide and mounting on a slide with an epoxy resin.[33]

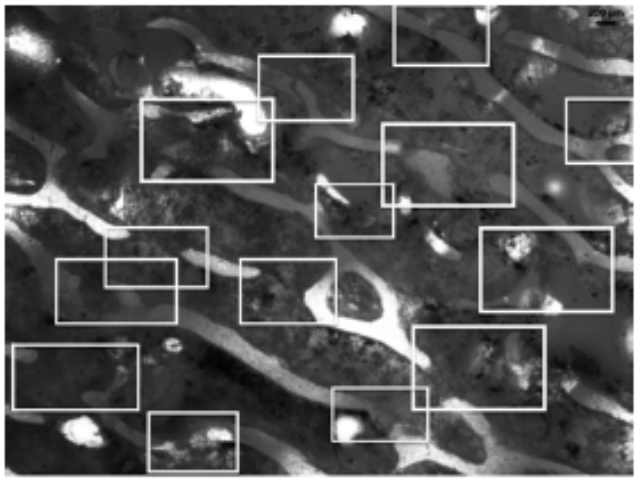

Fig.14 - Microstructure investigation of bovine cancellous bone. [33]

Before the micro analysis, the bone does not appear to experience shear stress. However, from fig.s4, the parallel lines of break (highlighted by rectengle) is found obviously inside bone, which means the specimen undergone shear. [33]

2.4.4. Limitations and modification

The conventional Split Hopkinson Pressure Bar apparatus generally allows the dynamic test between 102~104 s-1[27]. However, soft materials with lower strain rates, intermediate strain rate range 100~ 102 s-1, can give not enough data. [28]. At this kind of intermediate strain rate range, long enough loading duration is required to investigate large deformations in specimen, because

the soft materials, such as rubber, plastic and foam materials, generally shows large deformation. [28] The incident wave, that contains low amplitudes and long duration, does not be provided by a conventional SHPB. But there are some proper modifications for soft materials, that needs to be done at intermediate strain range, and those methods may allow to obtain sufficient data from SHPB. [23] And also because of the mismatch of impedance and wave reflection, the specimen is also subjected to a repeated loading condition. To get more better dynamic stress equilibrium and also a constant strain rate deformation and sufficient and precise transmitted signal for better stress-strain data.

Nemat-Nasser et al. [34] designed a momentum trap for a specimen to be subjected to only single stress pulse. Coaxially tube along the incident bar is applied. From the momentum trap an impedance is captured over 90% from the reflected wave.[34] The modification by momentum trap prevents any considerable reloading of the specimen. [34]

Chen and Song[23] also use the similar way with Nemat Nasser's[34] application, but a large coaxial mass, referred as 'a rigid mass'(Fig.15), is the differnece.

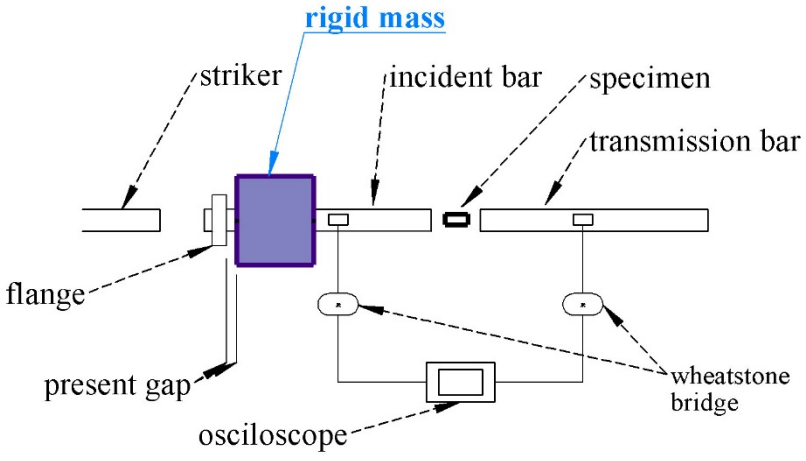

Fig.15 - A 'rigid mass' modification for soft material.(adapted from [23])

The rigid mass is applied instead of the tuve for matching the impedance. When the reflected pulse is returning, and tensile pulse whch is running up the bar to the specimen makes the end point of the incident bar is pulled away fromt eh spcimen. Hence, no further loading takes place.[23]However the mehod requires a high accuracy of setting striker speed and the gap of the rigid mass, which is not suitable for repetitive experiment.

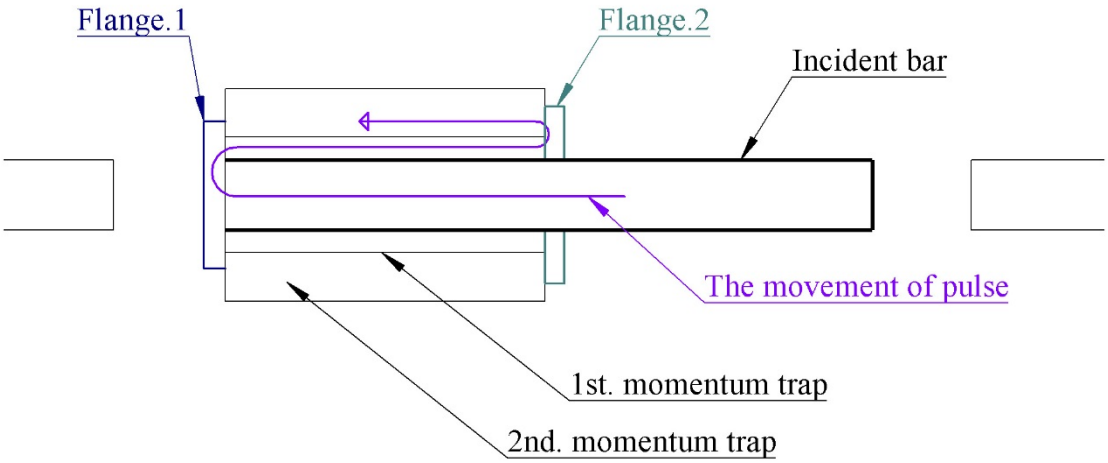

Fig.16 - modification from M.prot (, adapted from [33])

M.prot, et al[33] modified more from the previous methods. Two momentum traps are applied to captrue the wave of reflection. There are two momentum traps (rigid mass) and two flanges in Fig.S6. With tubed shape, 2nd momentum trap elclose the 1st one. When the incident bar impacts a specimen, the reflection wave from the specimen travels through the incident bar and then reaches ‘flange 1’ (Fig.16.) Then it propagates to the momentum traps, though 2nd one covers 1st one, it functions like two sequential traps. Two momentum traps setting allows a single specimen loading event at a predetermined velocity. And precise initial gap setting, which was problem for

repetitive experiments, is not required. From the result between signal history and high speed camera record, before second reflection wave reaches the specimen, the bar is apart from the specimen already, which means that there is only single loading event with the modification. [33] Though there are little unwanted effect, 3% displacement of a signal pak, however, the tandem traps are great modification of Split Hopkinson Pressure Bar experiment for the soft material including bone material. [33]

Fig.17 - Split Hopkinson Pressure Bar apparatus in the lab 105 in SBU.

Chapter 3 EXPERIMENT

A 3D printing technique, reviewed at chapter 2, is to manufacture 3d haptic model with CAD(Computer Aided Design) software. 2D printing concerns about only X and Y axis, on the other hand, the 3D printing expands to the Z axis. The variety of selection of material to print is an advantage of 3D printing technique, and PLA(Poly Lactic Acid), also reviewed on chapter 2, is also one of the them. Not only 3D printing technique, but also PLA is also being utilized to lots of industries because of its great properties and functionalities, such as high mechanical strength, good barrier properties and good appearance.[10] [14] Even the usage of PLA reaches the bio medical area, for example pins for ligament attachment and rods and pins in bone because of its low toxicity. [15]

A Fused Deposition Modelling (FDM) is one of the famous 3D printing technique. A filament, which is the material we use such as PLA or ABS (Acrylonitrile Butadiene Styrene), is fed through a heated part and get molten. The molten filament is going through a nozzle, and then deposited on a plate for construction. The printer is fabricating sliced cross section of the product with conversion from the CAD file. The head, having the nozzle emitting the molten material, moves X and Y direction and give off the molten filament with a predetermined thickness of layer. If the printer finishes a layer, it moves vertically to z axis with the predetermined height, and then printing out the next slice on top of the previous layer.The printed layer is rapidly solidifies, and the next layer is extruded on the previous printed layer.

3.1. Preparation of specimen

To prepare the printed PLA specimen, 'Replicator 2' 3D printer is used, which is Fused Deposition Modeling printer manufactured by 'Makerbot[tm].' The important features of the printer are described below.

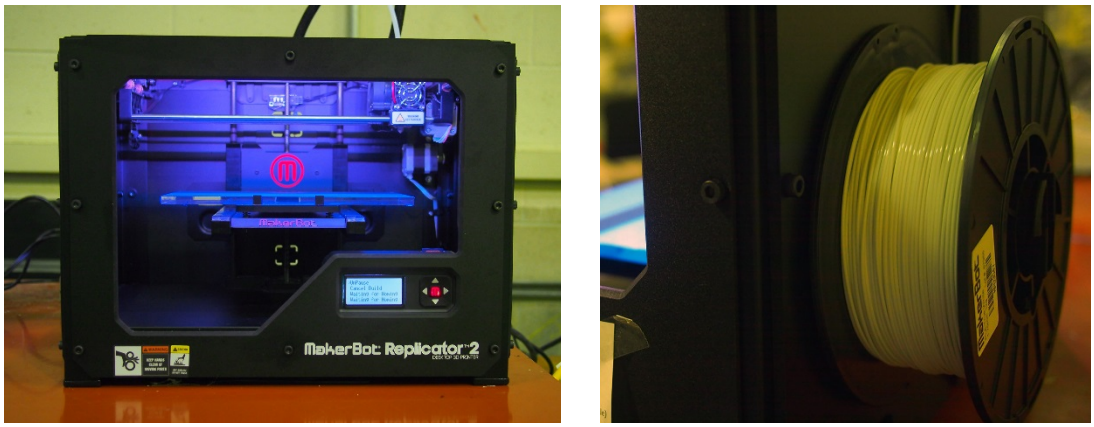

Fig.18 - (a) 3D printer, 'replicator 2', and (b) PLA filament.

Build volume (LxWxH)	28.5 x 15.3 x 15.5 cm ; 11.2 X 6.0 X 6.1 in
Filament Material	PLA
Layer resolution	100 microns [0.0039 IN]
Nozzle diameter	0.4 mm; [0.015 IN]

Tab.1 - The features of 3D printer 'replicator 2'

The purpose of this research begins from the assumption that the 'printed PLA' has a different property from the property of solid original PLA. To investigate the property of printed PLA, basic quasi-static tensile and compression tests were done. A 'Solidworks,' CAD software, was used to design 3D modelling of specimen. (exported to '.stl' format)

As a specimen for the tensile test, dog-bone specimen(fig.19) was prepared via 3D printer.

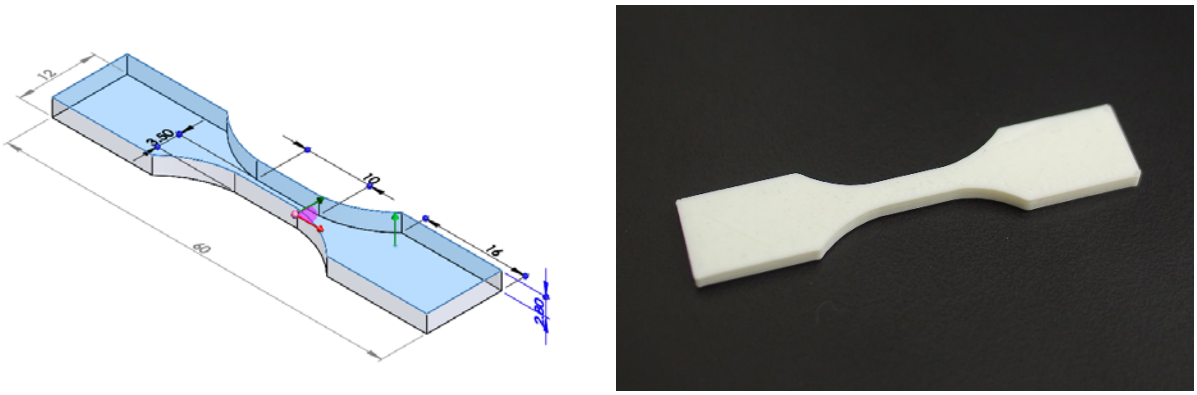

Fig.19 - (a) A schematic of dog-bone specimen (unit : mm) and (b) A printed dog-bone specimen.

From the setting of 3D printer, the amount how much fill inside of the material, referred to ‘in-fill ,' was set to 100%, which means that the dog-bone was filled perfectly with PLA. First of all, the printer draw (or extrude) the line for shell of the layer, and then it fills molten PLA based on the ‘in-fill’ setting programmed. Number of shell line was set to 2.

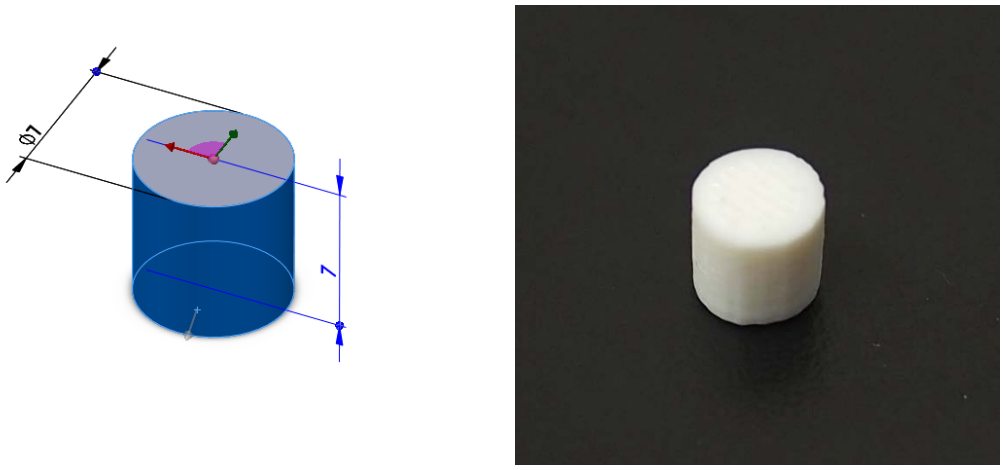

Fig.20 - (a) A schematic of cylinder (unit : mm) and (b) an output from the 3D printer.

For the compression test, solid cylinder was prepared by 3d printer. The thickness of the layer would be also controlled from the original software ‘makeware,’ which is for conversion of CAD

files(.STL format) to printer's original format(.X3G) that haves information of cross-section layers of 3D model.

Layer height	0.1 mm
Number of shell	1
Temperature of extruder	230 °C
Speed while extruding	80 mm/s

Tab.2 - The 3D printer setting for preparation of specimen.

For better output quality, layer height was set to the least thickness, 0.1mm, and 'speed while extruding' is also lowered to the 80 mm/s from 90 mm/s.

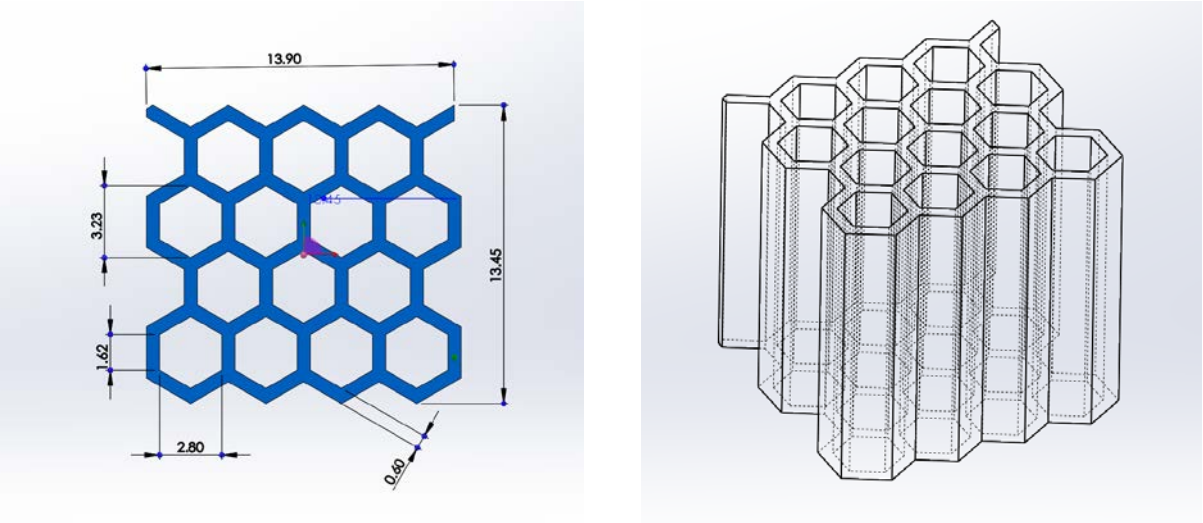

Fig.21 - A schematic of Honeycomb cellular cube. (Unit : mm / height : 13.45 mm)

As a representative of cellular material, honeycomb cube is designed for compression test. The selection of the length was chosen as similar as perfect cube, but for avoiding to cut the hexagonal shape on the middle, it was altered little. (13.90 x 13.45 x 13.45 mm) (Fig.21) And for further

dynamic test with Split Hopkinson Pressure Bar, the cress sectional area was set below the diameter of the bar.

Fig.22 - Honeycomb Cellular cube fabricated by 3D printer.

To find out general modulus of elasticity of printed PLA, tensile tests and compression tests were performed by ‘Tinius Olsen 1000’ compression-tension experiment tool.

Fig.23 - (a)‘Tinius Olsen’ apparatus and (b) camera preparation.

And to keep investigating apparent deformation of specimen, dslr camera was mounted on tripod as same level as a specimen on tester. And with same time interval, pictures were collected and could be matched with the stress and strain data.

3.2. Procedure of experiment

The goal of the experiment is to characterize the property and a mechanical behaviour of printed PLA from quasi-static compression and tensile test, and analyzing the behaviour of printed honeycomb cube under compression. And also finite element analysis is conducted for the comparison of deformation between simulation and real experiment via ‘Abaqus.’

First of all, to find out general property of printed PLA, the tensile test of dog-bone specimen was performed with 3 different speeds; 0.01, 0.05 and 1 in/min respectively. Eight dog-bone specimen were prepared by 3D printer, and a gauge length of dog-bone specimen was set to 10 mm. (Fig.19) The compression test of the printed cylinder was performed at the speed with 0.01, 0.05 and 1 in/min, respectively. All 6 cylinders were investigated. To find out visible indication, by the prepared camera (Fig.23), photos were taken at fixed interval on every experiment. From the result of the tensile and compression test, stress-strain curve was obtained as well as young’s modulus of printed PLA. The quasi-static compression test of honeycomb from 2 different in-plane directions is a major experiment in this paper. Based on the input information of printed PLA, the finite element analysis of the honeycomb structure performed via ‘Abaqus.’ A comparison between ideal and real behaviour of honeycomb that was exposed to quasi static compression is described in a next chapter.

Chapter 4 Result and discussion

4.1. Tensile test

Though eight dog-bone specimens were experimented for investigation of the property of printed PLA, most dog-bone samples break near shoulder. (fig.24)

Fig.24 - (a) An original dog-bone specimen, (b) dog-bone sample No.2 (0.05 in/min), (c) dog-bone sample No.3 (0.02 in/min), printed by 3D printer.

On a dog-bone sample No.2, which was tested with the speed of 0.05 in/min, not much elongation was observed. It shows very brittle behavior. The locations where the break happened were the near the border of gauge area (10mm), the stress-strain curve data from the test could not be used for the reference source of printed PLA. Though No.5 and 7's fracture were happen at middle of the gauge length, they were so brittle at speed of 0.05 and 0.1 in/min that difficult to get enough and precise data from the test.

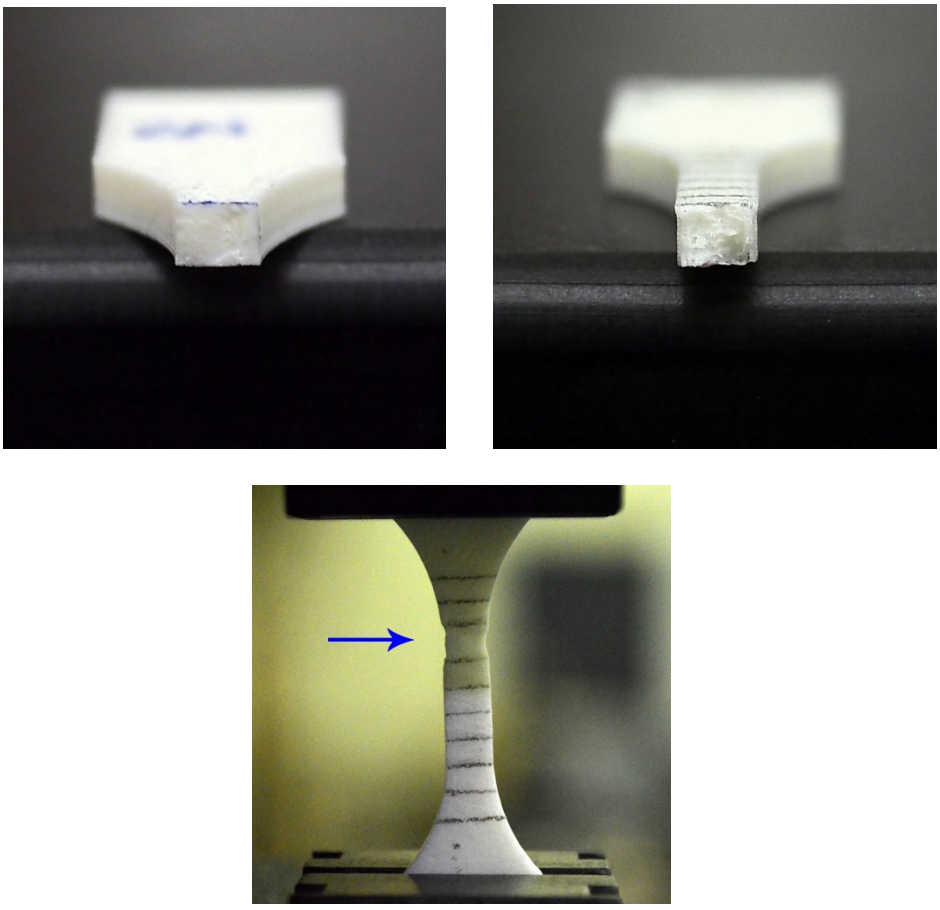

Fig.25 - (a) the cross-section view of dog-bone sample no.2, (b) sample no.3 and (c) the necking of sample no.3.

During the experiment, no.3 show the necking at low speed, 0.02 in/min. However, since the gauge area is not big enough and the fracture occurred near the end of the gauge length, the tensile test with dog-bone specimen of printed PLA was not successful. It is presumed that High porosity inside of printed material affected the brittle behavior of specimen. So for the proper future tensile test, setting the thicker gauge area up is suggested. Hence, the young's modulus obtained from the tensile test was not considered on this research.

4.2. Compression Test.

From the 6 cylinder experiments, on 0.01 in/min, 0.05 in/min, and 0.1 in/min respectively, stress-strain curves were obtained. Depending on the speed of the compression test, the results were varied, however, those stress-strain graphs showed similar shape, and for the representative of the property of printed PLA, the result at 0.05 in/min speed was chosen, due to the fact that the curve was an average of 6 tests.

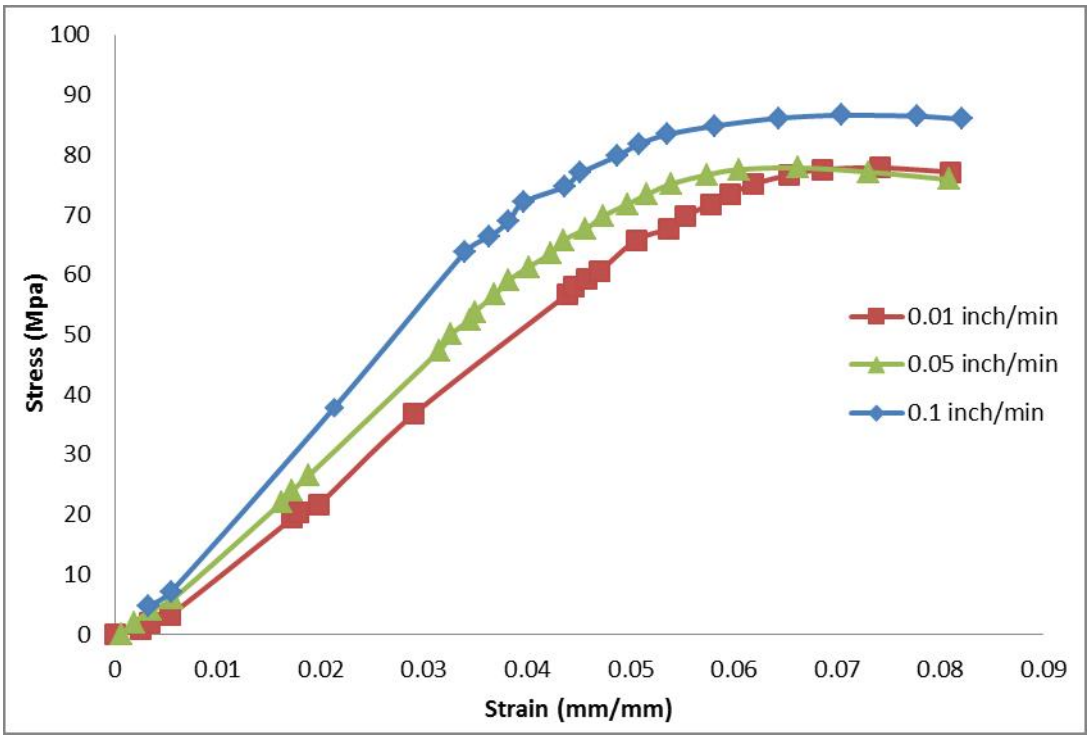

Fig.26 - The stress-strain curve obtained at speed 0.01 in/min (red square), 0.05 in/min (green triangle) and 0.1 in/min (blue rhombus), respectively.

Table.3 shows the property of the printed PLA obtained from the compression test of cylinders.

	Original PLA	Printed PLA
The modulus of elasticity (GPa)	3 - 3.5	1.67
Yield strength (MPa)	60 - 65	52.135
Density (g/cc)	1.235	1.1

Tab.3 - A comparison between original PLA and printed PLA.

The young's modulus of printed PLA is more than two times lower than original PLA, on the other hand, when it comes to the result of the yield strength of printed PLA does not show much difference, though lower than original PLA's yield strength. From the density of printed PLA, relative density of honeycomb foam was set as 47%.

4.3. Compression test on Honeycomb cellular structure

The hexagonal honeycomb cube consists of four cells in both x-direction and y-direction each. At speed of 0.1 in/min, two honeycomb cubes were tested with 'Y-direction' and 'X-direction.'(Fig.26)

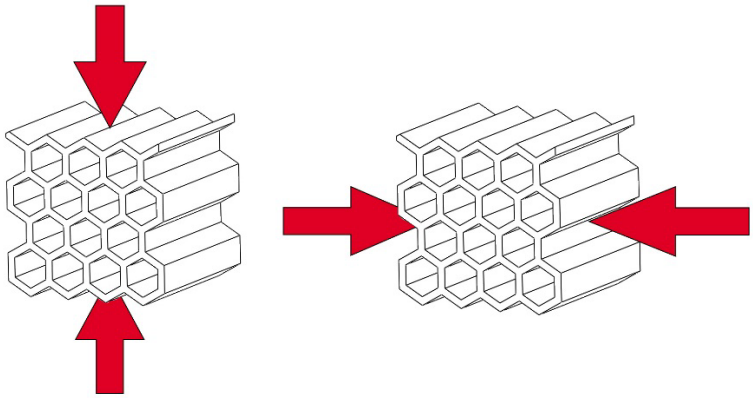

Fig.26 - A schematic of compression test: (a) Y-direction and (b) X-direction.

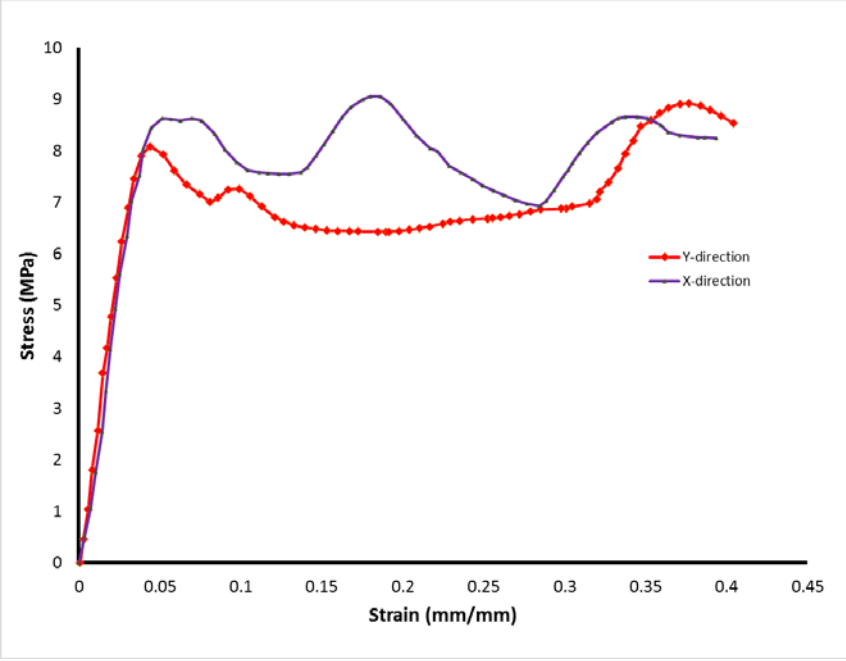

Fig.27 - A stress-strain curve from the compression test of honeycomb. Y-direction test is red rhombus line and the X-direction is referred as purple solid line.

From the stress-strain data (fig.27), the modulus of elasticity and yield strength of honeycomb cube, printed by PLA, are 248 MPa and 7 MPa, respectively. As expected, this result of young's modulus and yield strength is much lower than the solid cylinder specimen test. (1.6 GPa and 52 MPa respectively.) (Tab.3)

The yield strength and the stiffness of honeycomb, tested from both x and y direction, were matched. However, the shape of curves were different between x and y direction, which was due to the difference of localization behavior during deformation of cell walls.

4.3.1. Deformation in Y-direction

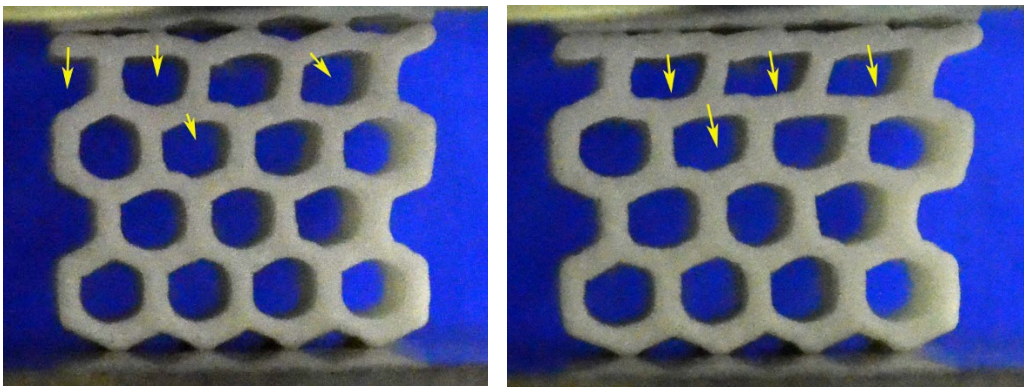

Fig.28 - Honeycomb under the strain of (a) 6.6% and (b) 11.3%.

In the fig.28, the yellow arrow described the movement of the corner of the hexagon wall. At the beginning of the collapse period, as shown in fig.28, the top end limbs of the specimen deformed firstly. Though the top location was fixed end, since the limbs were not in perfect hexagonal shape, first collapse took place on top. At (b), it was deformed perfectly flat.

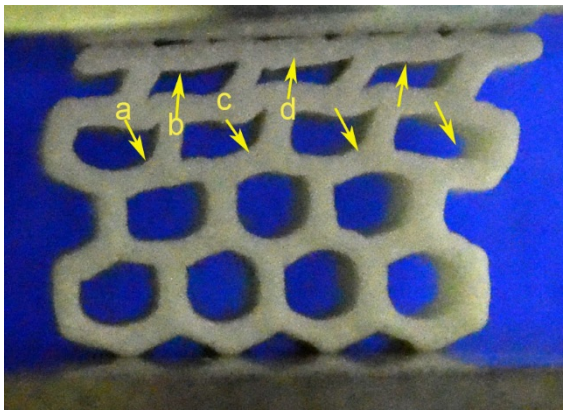

Fig. 29 - Under the strain of 20%. Y-direction compression test. Each small alphabets are referred to the corner of hexagon walls.

In fig.29, the corner ‘a’ and ‘c’ were going down during first raw was in the collapse period, on the other hand, corner ‘b’ and ‘d’ was going up, relatively..

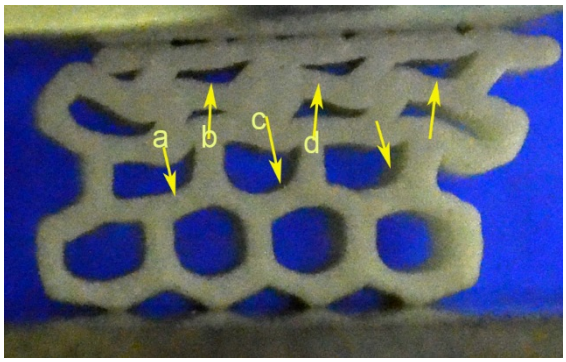

Fig.30 - Y-direction honeycomb under the strain of 32%.

By contact between first row and second raw, the localization band, which is cumulative zigzag band that collapse of cells happen in series, was shown.(fig.30) same as previous process, corner ‘a’ and ‘c’ was deformed downward, and ‘b’ and ‘d’ remained or relatively went up. With this repetitive collapse process of cells makes the localization band propagated.

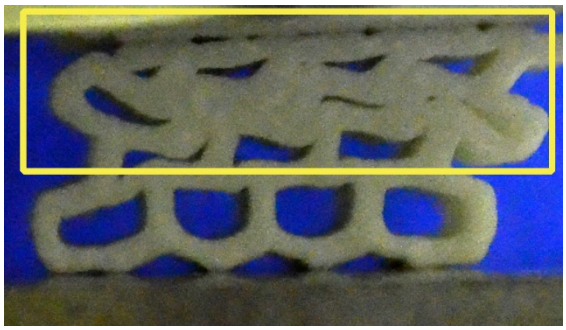

Fig.31 - Y-direction honeycomb under the strain of 40%. The yellow box referred to localization band.

At the 40% of strain, the localization band (which is described in fig.31) became denser, and moving down, on the other hand, the region below the localized band remained intact relatively.

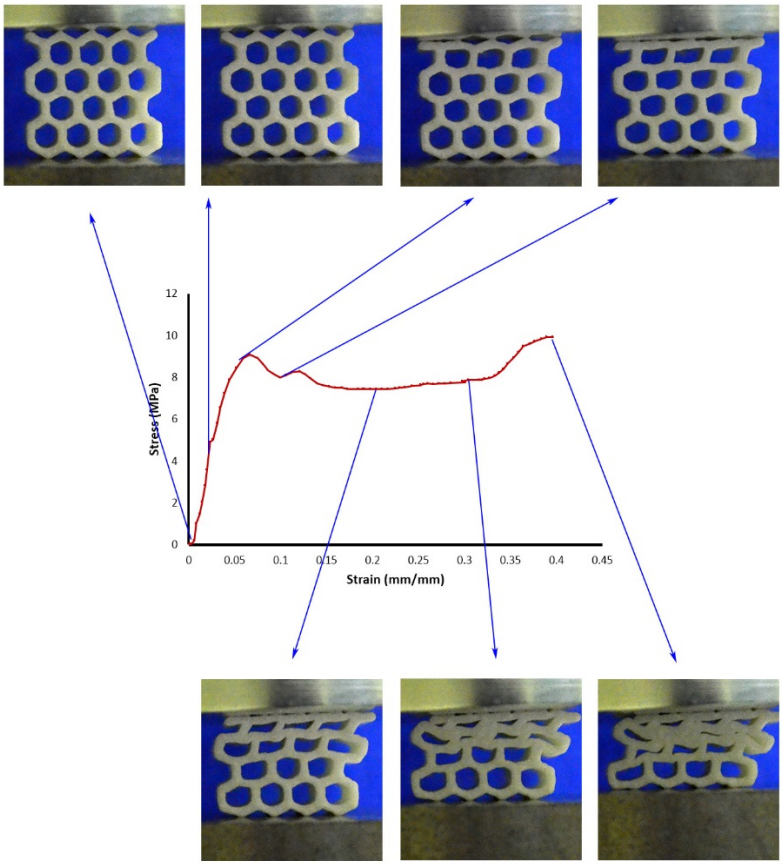

Fig.32 - The comparison with the pictures took by camera during deformation process; (a) 0%, (b) 1.8%, (c)6.6%, (d)11.3%, (e)20%, (f)32%, and (g)40%, respectively.

4.3.2. Deformation of honeycomb in X-direction

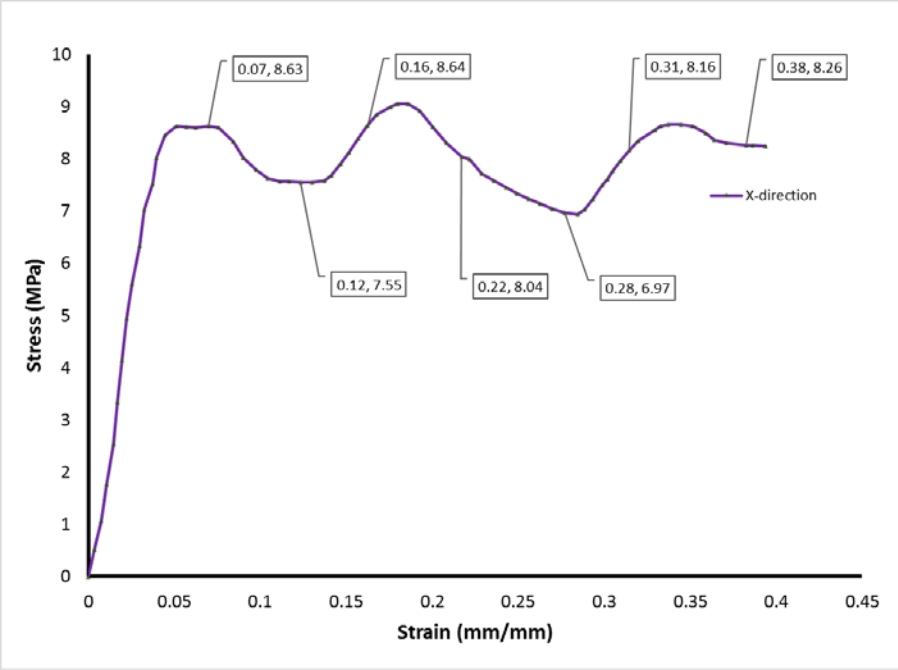

Fig.33 - A stress-strain curve of Honeycomb, X-direction. Described point referred to strain and stress.

The six points designated in Fig.33 was investigated for behavior of deformation of honeycomb(x-direction). Within the range of strain from 0 ~ 4%, the initial stiff, elastic behavior is shown.

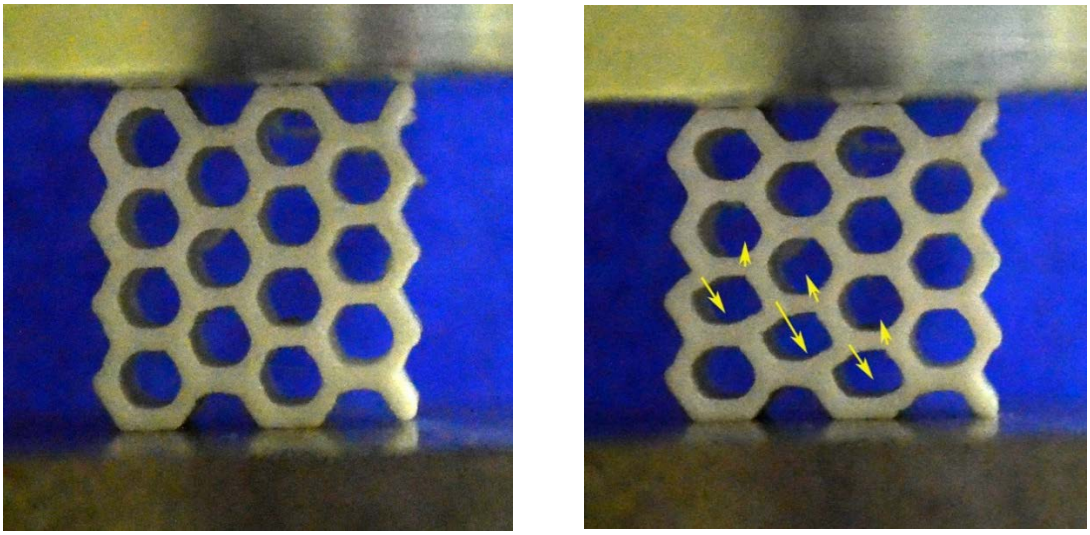

Fig.34 - (a) An original shape of the honeycomb structure before deformation, and (b) after yield point.(7%) in the x-direction.

After yield strain point, near the bottom end, collapse took place in a row. In the cell, where collapse was on going, left upper corner was going down, and right upper corner was raised relatively. With this mechanism, zigzag shaped front line is made in the honeycomb structure.

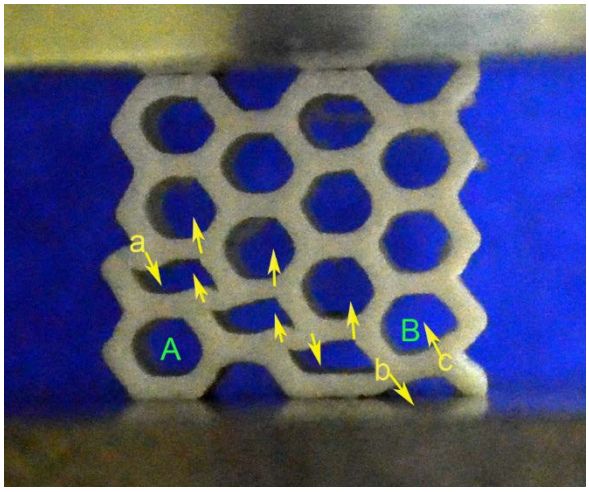

Fig.35 - The honeycomb under 12% of strain. The yellow lower case alphabet referred to the corner of cells. Upper case letter referred to the cell.

The fig.35 shows the progress of cell collapse. Until the line of cells crushed completely, other cells seemed intact. From the stress-strain curve (fig.33), at 12% strain the load remained steady, since the plastic collapse was proceeding. The corner ‘b’ in fig.35 almost touched the end, which is presumed that the imperfect structure below corner ‘b’ was weak to bear the stress. As the upper right corner of collapse row, the corner ‘c’ was raised with corner ‘b’ moved down. The ‘A’ cell was almost not deformed though located below the collapse line. And ‘B’ cell was being deformed as corner ‘c’ going up. From 14% strain to around 16% strain, the load was increased rapidly after collapse period of first row finished somehow.

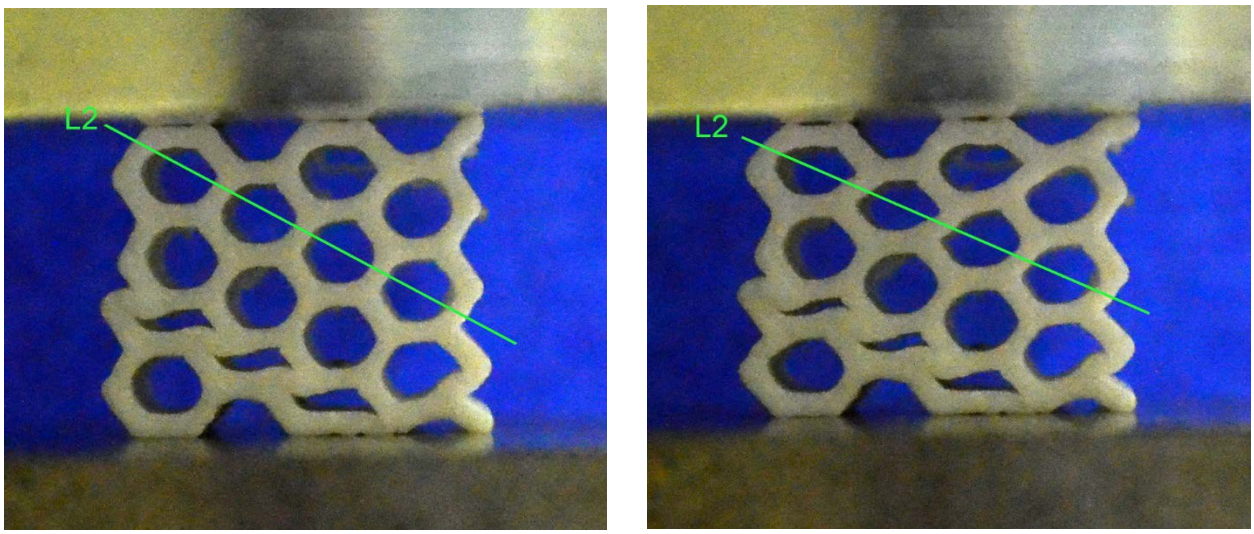

Fig.36 - The honeycomb under (a) (16%), and (b) (22%) of strain in x-direction.

After first line of cells collapsed completely, ‘L2’ row of cells was on set of the crush in fig.36. At 22% of strain, as the ‘L2’ line was under deformation, the stress was decreasing gradually.

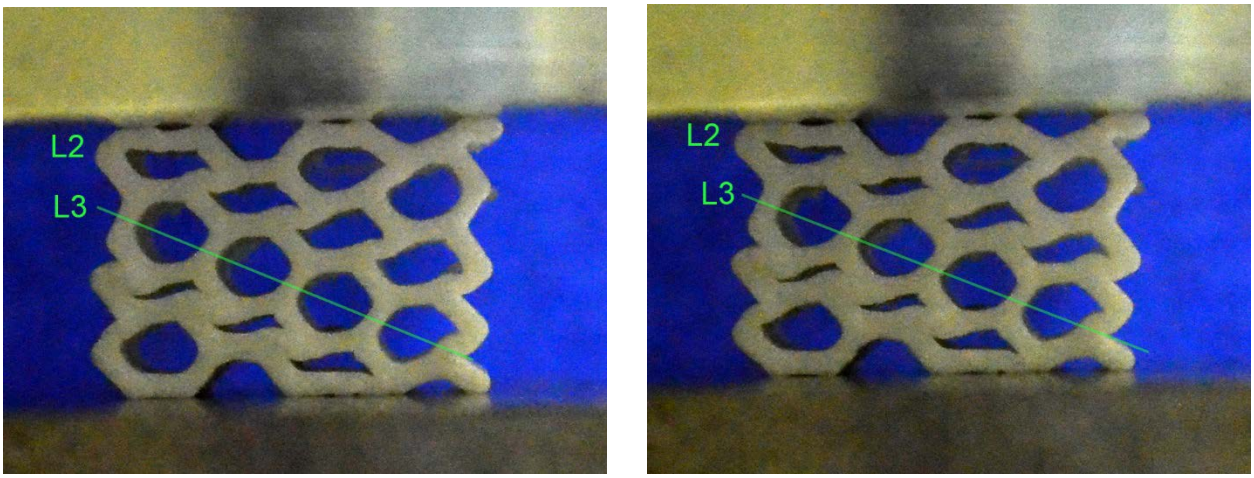

Fig.37 - The honeycomb under (a) 28% and (b)31% in x-direction.

On 28% of strain, ‘L2’ line (fig.37) almost collapsed. With ‘L2’line was collapsed fully, ‘L3’line (fig.37 (a)) was subjected to the deformation. In fig.r14 (b), as the cells in ‘L3’ line was resisting against the load, the stress was increasing in the stress-strain graph(fig.33). The result of the honeycomb in x direction test shows the repeated pattern, as a strain increased, the stress was

oscillated from 7 to 9 MPa, which was matched with the deformation propagation of the honeycomb specimen.

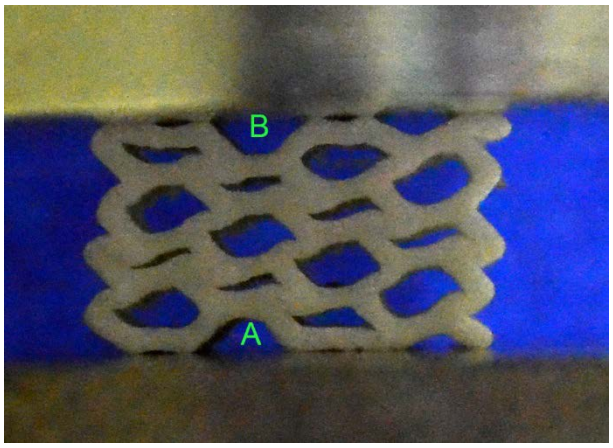

Fig.38 - The honeycomb under 38% of strain in x-direction.

On the contrary to the y-direction result, in the test of x-direction, the localization band were made separately near the top and bottom each. Though figuring out the exact reason is not possible in this experiment, some possibility could be presumed with observation of visible indication.

In Fig.38, the region ‘A’ and ‘B’ looks very stable. Three walls at ’A’ (or ‘B’) were supported by nearby hexagonal cells and the plate. So, from the region of A and B, the deformation could be propagated to nearby raw. Or, simply the difference of thickness of wall of cell could make separate row of collapse. And it is also possible that during the printing procedure, defect took place at only certain point.

4.5. Finite Element Analysis of honeycomb

Finite element analysis of honeycomb structure were made via 'Abaqus.' The properties of printed PLA from the result of cylinder specimen were used as the input value.

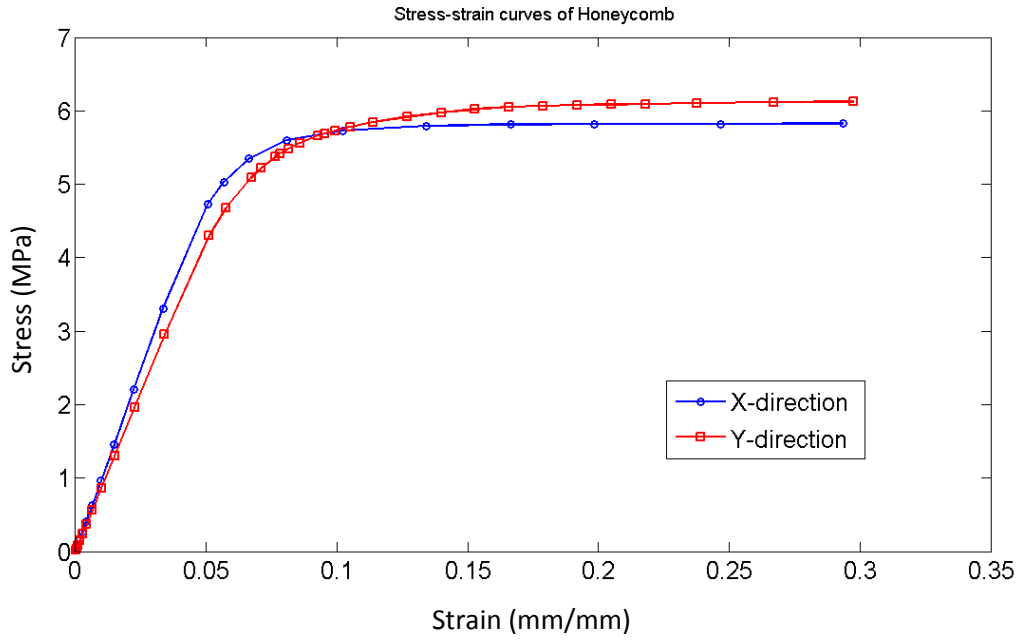

Fig.39 - stress-strain curve of honeycomb obtained from FEM.

The result of the finite element analysis shows that the stiffness is much lower than the result from the experiment. The discrepancy is originated from the thickness difference between CAD file and the printed specimen. When the specimen was prepared, the thickness of each wall was larger than the original CAD's, and the strength of honeycomb is highly related with the thickness of the wall. [20] Since the simulation used the property from original thickness (0.6mm), the result shown is understandable. The experiment showed oscillation of stress as the localization band propagates, on the other hand, from the simulation, after certain strain, 0.1 in the x-direction, it shows only flat plateau. Though in y-direction, the plateau initiates from 0.17 strain, the oscillation is not observed.

		Simulation	Experiment
X-direction	Yield strength (MPa)	3.8	7
	Elastic modulus, MPa)	98	248
Y-direction	Yield strength (MPa)	3.3	6.5
	Elastic modulus, MPa)	86.2	227

Tab.4 - The comparison of property between simulation and experiment.

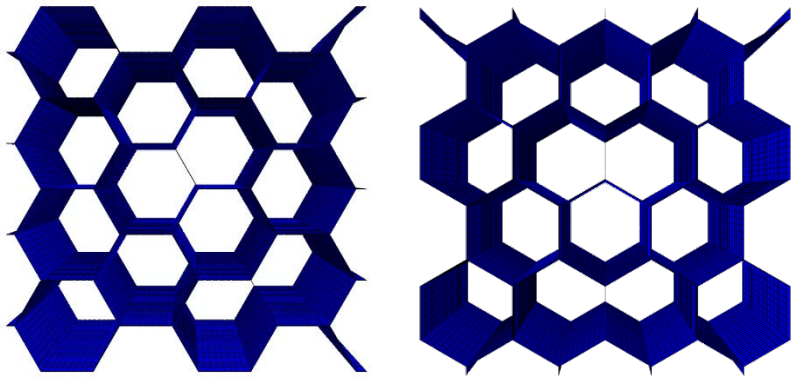

Fig.40 - The reference of honeycomb FEM image; (a) x-direction and (b) y-direction

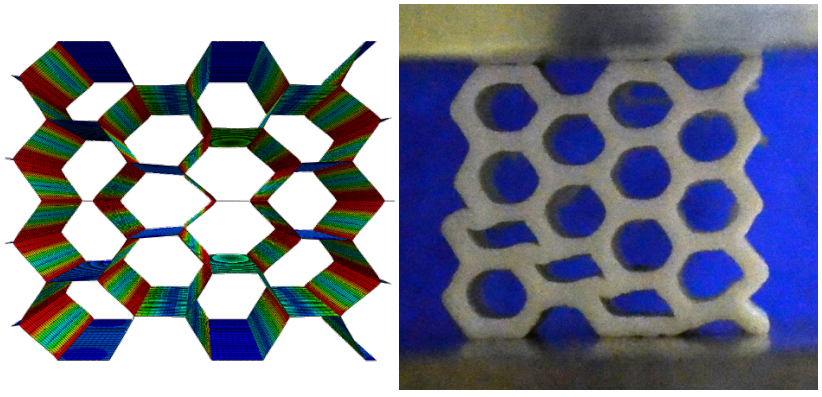

Fig.41 - (a) the simulation and (b) the experiment in x-direction under the 13% strain each.

However, the shape of deformation presented differently between the simulation and the experiment. In the fig.40 shows the difference of deformation between two under the strain of 13%. In fig.40 (b), the specimen form experiment was deformed only at a line of cells, on the other hand, in the FEM model, no collapse line exists. Through all length of axis, the deformation of all cells looks uniform.

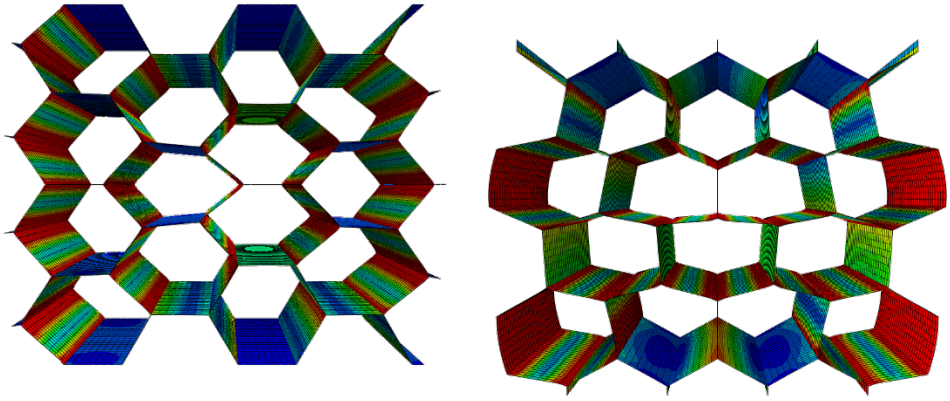

Fig.42 - The FEM image Under 30% of strain in (a) x-direction and (b) y-direction.

In the fig.42, which is the result under the strain of 30% in both directions, in x-direction the cell walls parallel to the compressive plate shown blue color, which means it is under less stress. In y-direction, a slight barrelling of the honeycomb is observed.

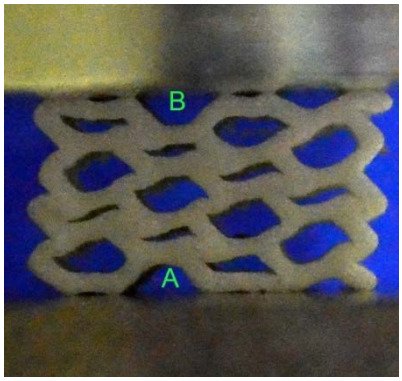

Fig.43 - The specimen from experiment under the strain of 38%.

In the experiment part, the stability of the region ‘A’ and ‘B’ (fig.43) was mentioned. In the simulation (fig.42 (a),) similarly the area, correspond to ‘A’ and ‘B ,' showed stable, as well.

Chapter 5 Conclusion

In the present work, Poly lactic acid (PLA) was used as a model system to investigate the deformation behavior of honeycomb foams in compression. Solid PLA tension specimens and foams made of PLA were fabricated using fused deposition 3-D printing technique. The solid PLA tension specimens were characterized for their densities and found to be about 10% lower in density as compared to their bulk counter parts. The honeycomb foams had a relative density of about 47%. The deformation mechanisms leading to the crushing of the honeycomb foams under compression were characterized. Furthermore, simple finite element models were developed to understand the observed deformation behavior of honeycomb foams.

References

[1] S. Bose, S. Vahabzadeh, and A. Bandyopadhyay, “Bone tissue engineering using 3D printing,” *Biochemical Pharmacology*, 2013.

[2] Dudek, P. "FDM 3D printing technology in manufacturing composite elements." *Archives of Metallurgy and Materials* 58.4, 2013.

[3] H. Tan and S. Qu, “Impact of Cellular Materials,” pp. 309–334, 2010.

[4] L. L. Hu and T. X. Yu, “Dynamic crushing strength of hexagonal honeycombs,” *International Journal of Impact Engineering*, 2010.

[5] http://www.epa.gov/lean/environment/methods/cellular.htm.

[6] Bijarimi, Mohd, Sahrim Ahmad, and Rozaidi Rasid. "Mechanical, thermal and morphological properties of PLA/PP melt blends." *International Conference on Agriculture, Chemical and Environmental Sciences*, 2012.

[7] E.M. Sachs, et al., Three-dimensional printing techniques, US Patent #5,204,055.

[8] Sachs, Emanuel, M. Cima, and J. Cornie. "Three-dimensional printing: rapid tooling and prototypes directly from a CAD model." *CIRP Annals-Manufacturing Technology* 39.1, 1990.

[9] Leigh, Simon J., et al. "A simple, low-cost conductive composite material for 3D printing of electronic sensors." *PloS one* 7.11, 2012.

[10] Masaki, Kazuo, et al. "Cutinase-like enzyme from the yeast Cryptococcus sp. strain S-2 hydrolyzes polylactic acid and other biodegradable plastics." *Applied and environmental microbiology* 71.11, 2005

[11] Conn, R. E., et al. "Safety assessment of polylactide (PLA) for use as a food-contact polymer." *Food and Chemical Toxicology* 33.4, 1995

[12] Datta, Rathin, and Michael Henry. "Lactic acid: recent advances in products, processes and technologies—a review." *Journal of Chemical Technology and Biotechnology* 81.7, 2006

[13] Hartmann, M. H. "High molecular weight polylactic acid polymers." *Biopolymers from renewable resources*. Springer Berlin Heidelberg, 1998.

[14] Lim, Jung Yul, et al. "Improvement of Flexural Strengths of Poly (L-lactic acid) by Solid-State Extrusion." *Macromolecular Chemistry and Physics* 202.11, 2001.

[15] Furukawa, Tsuyoshi, et al. "Structure, dispersibility, and crystallinity of poly (hydroxybutyrate)/poly (l-lactic acid) blends studied by FT-IR microspectroscopy and differential scanning calorimetry." *Macromolecules* 38.15, 2005.

[16] Brandrup, Johannes, et al., eds. *Polymer handbook*. Vol. 1999. New York: Wiley, 1999.

[17] Bastioli, Catia, ed. “Handbook of biodegradable polymers.” *iSmithers Rapra Publishing*, 2005.

[18] E. Hassan, Y. Wei, H. Jiao, and M. Yu, “Dynamic Mechanical properties and Thermal stability of Poly(lactic acid) and poly(butylene succinate) blends composites,” *JFBI, vol. 6,* 2013.

[19] Reid, S. R., and C. Peng. "Dynamic uniaxial crushing of wood." *International Journal of Impact Engineering* 19.5, 1997.

[20] M. R. Said and C.-F. Tan, “Aluminium honeycomb under quasi-static compressive loading: An experimental investigation.” *Suranaree Journal of Science & Technology,* vol. 16, no. 1, 2009.

[21] Z. Zou, S. R. Reid, P. J. Tan, S. Li, and J. J. Harrigan, “Dynamic crushing of honeycombs and features of shock fronts,” *International Journal of Impact Engineering,* vol. 36, no. 1 , 2009.

[22] Ruan, D., et al. "In-plane dynamic crushing of honeycombs—a finite element study." *International Journal of Impact Engineering* 28.2, 2003.

[23] B. Song and W. Chen, “Split Hopkinson pressure bar techniques for characterizing soft materials.” *Latin American Journal of Solids and Structures,* vol. 2, no. 2, 2005.

[24] G. T. Gary. “Classic Split Hopkinson Pressure Bar testing, mechanical testing and evaluation, metals handbook. American Society for Metals,” 8: 462–476, 2000.

[25] Song, Bo, et al. "Confinement effects on the dynamic compressive properties of an epoxy syntactic foam." *Composite structures* 67.3, 2005

[26] Song, Bo, et al. "Temperature effects on dynamic compressive behavior of an epoxy syntactic foam." *Composite Structures* 67.3, 2005.

[27] Meyers, Marc A. “Dynamic behavior of materials.” *John Wiley & Sons,* 1994.

[28] Zhao, Han, and Gerard Gary. "A new method for the separation of waves. Application to the SHPB technique for an unlimited duration of measurement."*Journal of the Mechanics and Physics of Solids* 45.7, 1997.

[29] Gallina, Felipe, and Marcilio Alves. “Design of a Split Hopkinson Pressure Bar.” *EPUSP*, 2004.

[30] Song, B., and W. Chen. "Energy for specimen deformation in a split Hopkinson pressure bar experiment." *Experimental mechanics* 46.3, 2006.

[31] Johnson, Timothy Paul Mahal. “High strain rate mechanical characterization of trabecular bone utilizing the split-Hopkinson pressure bar technique.” *Diss. Massachusetts Institute of Technology*, 2005.

[32] G. T. R. Gray III, “High-strain rate testing of materials: The Split-Hopkinson Pressure Bar,” pp. 1–15, 2012.

[33] Prot, M., T. J. Cloete, and S. Pattofatto. "Dynamic compression and recovery of cancellous bone for microstructural investigation." *EPJ Web of Conferences*. Vol. 26. EDP Sciences, 2012.

[34] Nemat-Nasser, Sia, Jon B. Isaacs, and John E. Starrett. "Hopkinson techniques for dynamic recovery experiments." *Proceedings of the Royal Society of London. Series A: Mathematical and Physical Sciences* 435.1894, 1991.